 doi:10.20944/preprints202204.0140.v1

Article

A facile fabrication of CdSe/ZnS QDs -block copolymer brushes modified graphene oxide nanohybrid with temperature-responsive behavior

Yajiao Song, Hongcui Yu, Xiaohui Wang, Jinglin Liu* and Jinghai Liu*

College of Chemistry and Materials Science, Inner Mongolia Key Laboratory of Carbon Nanomaterials, Key Laboratory of Natural Products Chemistry and Functional Molecular Synthesis, Inner Mongolia Minzu University, Tongliao 028000, China

Abstrsct: In this work, thermo-responsive block copolymer brushes modified graphene oxide (GO) nanohybrid was fabricated successfully via the host-guest interaction between β-cyclodextrin functionalized GO and azobenzene-terminated PNIPAM-*b*-P(St-*co*-MQ). The block copolymer was synthesized using reversible addition fragmentation chain transfer (RAFT) polymerization based on the monomers of N-isopropylacrylamide (NIPAM), 5-(2-methacryloyl-ethyloxymethyl) -8-quinolinol (MQ), styrene (St) and an azobenzene functional RAFT agent. The 8-hydroxyquinoline units containing in the block polymer can coordinate with CdSe/ZnS quantum dots(QDs) to form a CdSe/ZnS QDs-block copolymer brushes modified graphene oxide fluorescence nanohybrid (QDs/polymer/GO fluorescence nanohybrid) and the resulting fluorescence nanohybrid had a robust temperature responsive property which result from the change in the PNIPAM conformation in the block copolymer on the surface of GO.

Keywords: graphene oxide; nanohybrid; temperature-responsive

1. Introduction

Graphene, as a youngest two-dimensional nanomaterial, has sparked an enormous interest in the field of materials science since the single-atom thickness graphene was fabricated successfully[1,2]. Graphene oxide (GO), as a derivative of graphene, which easily obtained from graphite, has also gained considerable attention because of its abundant oxygen-containing functional groups on the basal plane and the edges of graphene[1-9]. These various oxygen-containing organic moieties such as carboxyl, hydroxyl, and epoxy groups provide GO with excellent water dispersibility[4]. What's more, the presence of these reactive groups make GO to be highly attractive for easily tailored and for the development of new advanced materials[4,6]. Recently, the concept of “organic/inorganic nano-composites” has been extended to the field of polymer-GO hybrid and achieved success. Numerous effect methods about the fabrication of polymer-GO hybrid have been reported in the past few years[10-20]. In brief, these approaches can be classified into two routes：covalent and non-covalent. In the covalent routes, “grafting from” and “grafting to” are two common strategies to grow polymer brushes on the surface of GO[10]. The “grafting from” technique which use initiator-functionalized GO as

 doi:10.20944/preprints202204.0140.v1

precursor for polymerization include atom transfer radical polymerization(ATRP) and reversible.addition-fragmentation chain transfer (RAFT) polymerization[11-12]. According to “grafting to” methods, the functional polymers is directly covalent on the surface of GO. Esterification[13], click chemistry[14], nitrene chemistry[15,16], amidation[17] and radical addition[18] are common “grafting to” methods. Besides, the non-covalent modification such as H-bonding[19] and π-π stacking interaction on GO surface[20] has also been viewed effective methods to prepared polymer-GO hybrid. In short, all the above methods have virtue and shortcoming. For instance, the “grafting to” methods could afford well-defined polymers to modify GO, but the “grafting to” methods has low yields and grafting density as compared with “grafting from” technique because of the serious steric hindrance from the attached polymer brushes[21].Conversely, “grafting from” methods provided GO hybrid with high grafting density and rough control over composition, however, multi-step synthesis were ordinarily necessary[21]. When a comparison is made between covalent and non-covalent routes, it is found that the covalent attachment has the potential of disrupting the conjugated structure of GO, leading to compromised physical properties of GO. But the modification of GO using non-covalent technique could retain the conjugated structure of GO after modification[12].

Herein, we developed a novel strategy to construct QDs/polymer/GO fluorescence nanohybrid based on 8-hydroxyquinoline ligand-containing block copolymer functionalized GO. As shown in Scheme 1, the block copolymer PNIPAM-*b*-P(St-*co*-MQ) was synthesized by the RAFT polymerization using the monomers of NIPAM, MQ, St and a azobenzene functional RAFT agent as raw materials. In addition, the mono-[6-(2-aminoethylamino)-6-deoxy]-cyclodextin (EDA-CD) modified GO hybrid was prepared via the reaction between amino group of the EDA-CD and carboxyl group on surface of GO. Finally, the QDs/polymer/GO fluorescence nanohybrid was fabricated by the host-guest interaction between β-cyclodextrin modified GO and azobenzene-terminated block copolymer, meanwhile the CdSe/ZnS QDs modified on the block copolymer brushes by the coordination between MQ units and CdSe/ZnS QDs (see Scheme 2). In this work, we choose the CdSe/ZnS QDs to coordinate with MQ because of their unique electrical and optical properties that depend on their size and shape[18]. In result, the resulting hybrid has a robust temperature responsive property which was resulted from the change in the PNIPAM conformation in the block copolymer brush on the surface GO (see Scheme 2).

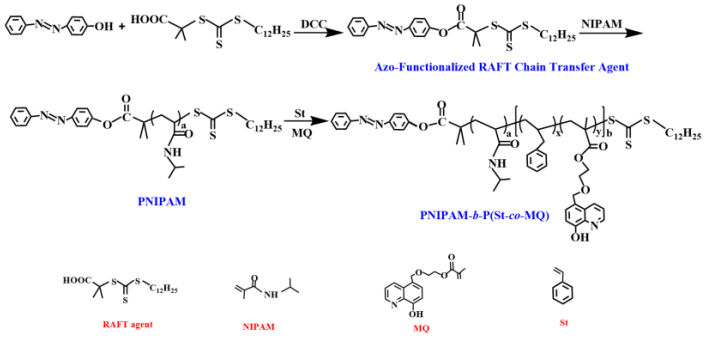

Scheme 1 Schematic illustration for preparation of PNIPAM-b-(St-co-MQ)

 doi:10.20944/preprints202204.0140.v1

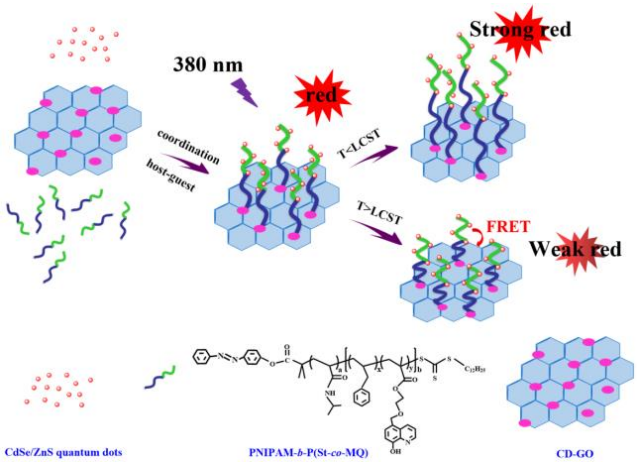

Scheme 2 Schematic illustration for preparation of QDs/polymer/GO fluorescence nanohybrid.

2. Experimental

2.1 Materials

N-isopropylacrylamide(NIPAM, 99%) was purchased from Aldrich and recrystallized in hexane before use. 2,2-Azoisobutyronitrile (AIBN) was purchased from Macklin and recrystallized from ethanol (95%) before use. CdSe/ZnS QDs was purchased from Xingshuo Nanotechnology Co., Ltd. Graphene oxide[23], 2-[(dodecylsulfanyl) carbonothioy lsulfanyl] propanoic acid (RAFT agent)[24], 5-(2-methacryloylethyloxy-methyl)-8-quinolinol(MQ)[25] and mono-[6-(2-aminoethy -lamino)-6-deoxy]-cyclodextin(6-NH_2-β-CD)[26] was synthesized according to literature procedures. All other reagents were purchased from commercial sources and used as received.

2.2 Preparation of thermo-responsive block polymer PNIPAM-*b*-P(St-*co*-MQ)

In order to synthesize azobenzene (Azo)-terminated thermo-responsive block polymer PNIPAM-*b*-P(St-*co*-MQ), we prepared a novel azobenzene functionalized chain transfer agent (Azo-RAFT agent) as follows[27]: Brieflly, 80 mL dry dichloromethane was loaded in a 100 mL round bottom flask, followed by adding 0.36 g RAFT agent and 0.2 g 4-phenylazophenol. After stirring for 1 h in an ice bath with nitrogen, the dichloromethane solution of DCC(0.42 g) and 4-(N,N-dimethylamino) pyridine (DMAP) (0.24 g) were added into the mixture and the reaction was carried out at room temperature for 24 h. After that, the filtrate was collected and concentrated, dissolved in chloroform and washed with water several times. Then the organic layer filtered and concentrated repeat after dried with $MgSO_4$ overnight.

Typical procedure employed for the synthesis of PNIPAM was as follows: a three-necked round-bottom flask was charged with NIPAM (2 g), AIBN (4 mg), Azo-RAFT agent (4 mg) and THF (6 mL). The mixture was degassed by three freeze-pump-thaw cycles and then sealed under vacuum. After the polymerization was conducted at 75 ºC for 12h, the product was centrifuged and washed with diethyl ether for several times. At last, the polymer PNIPAM was obtained after drying in a vacuum oven overnight at room temperature.

 doi:10.20944/preprints202204.0140.v1

The Azo-terminated block polymer PNIPAM-*b*-P(St-*co*-MQ) was synthesized as follows: PNIPAM(600 mg), MQ(140 mg), AIBN(8 mg) and DMF(6 mL) were placed in a three-necked round-bottom flask. After degassed by three freeze-pump-thaw cycles, the polymerization was conducted at 75°C under vacuum for 12 h, then the mixture was centrifuged and washed with diethyl ether for several times. The Azo-terminated block copolyme rPNIPAM-*b*-P(St-*co*-MQ) was obtained after drying in a vacuum oven overnight at room temperature.

2.3 Preparation of β-cyclodextrin modified GO(CD-GO)

The β-cyclodextrin modified GO(CD-GO) was synthesized as follows[26]: NaOH (5.0 g), chloroacetic acid (5.0 g) and GO(0.1 g) were dispersed in 100 mL deionized water and ultrasonicated for 2h in a ice-bath. Then the resulting products(COOH-GO) were centrifuged and washed with deionized water for several times and then concentrated in vacuo. The β-cyclodextrin modified GO(CD-GO) was prepared by the amidation between amino group of 6-NH_2-β-CD and carboxyl groups on the surface of GO-COOH. Briefly, GO-COOH (0.1 g) was dispersed in 100 mL deionized water followed by adding 115 mg 1-ethyl-3-(3-dimethy laminopropyl) carbodiimide hydrochloride(EDC) and 60 mg N-Hydroxy-sulfosu ccinimide(NHS). After ultrasonicated for 30 min at room temperature, 0.2 g 6-NH_2-β-CD was added followed by an additional reaction for 24 h. After the reaction was complete, the above mixture was centrifuged and washed with deionized water respectively, then CD-GO hybrid was obtained after drying in vacuum overnight at room temperature.

2.4 Preparation of QDs/polymer/GO fluorescence nanohybrid

A round-bottom flask containing 5mL deionized water was charged with PNIPAM-b-P(St-co-MQ) (30 mg), CD-GO (10 mg) and CdSe/ZnS QDs (20 μL, 4.17 mg·mL^{-1}). After ultrasonicated for 30 min, the reaction was conducted at room temperature for 36 h, then the above mixture was centrifuged and washed with deionized water for several times. After that the resulting QDs/polymer/GO fluorescence nanohybrid was obtained after drying in vacuum for 12h.

2.5 Measurements

^{1}H NMR spectra were recorded on a Bruker AV300 NMR spectrometer (resonance frequency of 500 MHz for ^{1}H NMR) operated in the Fourier transform mode. The molecular weight of copolymer was estimated at a flow rate of 1.0 mL min^{-1} at 25 °C by gel permeation chromatography (GPC) on a Waters instrument (Waters Corporation, USA), using DMF as eluent, and the molecular weight was determined vs polystyrene standards. FT-IR spectra were obtained using a Magna 560 FT-IR spectrometer. Raman spectra were recorded on a Renishaw 1000 model confocal microscope. Transmission electron microscopy (TEM) images were captured by JEOL-2021 electron microscope. Thermogravimetric analysis (TGA) was carried out with a PL thermo-gravimetric analyzer (Polymer Laboratories, TGA1000, UK) at a heating rate of 10 oC min^{-1} and nitrogen was used as the purging gas. UV-vis absorption spectra were monitored using SHIMADZU -UV-

 doi:10.20944/preprints202204.0140.v1

2550-UV-visible spectrophotometer (the range from 200 to 700 nm). Fluorescence measurements were performed on a Cary Eclipse fluorescence spectrometer. The fluorescence emission spectra were measured in 400-700 nm with an excitation at 380 nm.

3. Results and discussion

3.1. Characterization of QDs/polymer/GO fluorescence nanohybrid

In order to synthesize Azo-terminated block polymer PNIPAM-*b*-P(St-*co*-MQ), we designed and prepared a novel Azo functionalized chain transfer agent (Azo-RAFT agent) firstly. Figure 1 shows the ^{1}H NMR spectra of RAFT agent and Azo-RAFT agent in $CDCl_3$. The peak assignments have been marked in Figure 1. As shown in Figure1a, the chemical shift located at 3.20 ppm for the RAFT agent is attributed to the proton on the methylene group near the trithiocarbons. The signals at 1.66 ppm is assigned to the proton on two methyl groups near the carboxyl group. The signals at 1.60-1.11 ppm is assigned to the proton on the methyl group at the end of the RAFT agent[24]. While some new signals appear in the spectra of Azo-RAFT agent, As seen Figure 1b, the signals at 7.22-7.27(d, 2H, azobenzene-Hα), 7.46- 7.54(m, 3H, azobenzene-Hγ) and 7.87-7.96 ppm (m, 4H, azobenzene-H$_\beta$) are the protons of azobenzene[27]. As expected, the ^{1}H NMR spectra of the above chain transfer agents testify the successful synthesis of RAFT agent and Azo-RAFT agent.

The Azo-terminated block polymer PNIPAM-*b*-P(St-*co*-MQ) was prepared based on the monomers of NIPAM, St and MQ though the RAFT polymerization. Figure 2 shows the ^{1}H NMR spectra of PNIPAM and PNIPAM-*b*-P(St-*co*-MQ) in $CDCl_3$. As shown in Figure 2a, the signal at 4.0 ppm which is assigned to the O=CNH proton the PNIPAM illustrate the polymer PIPAM was prepared successfully[28]. As seen in Figure 2b, the signal at 6.40-7.10 ppm are protons of phenyl ring and the signals at 8.5 and 8.7 ppm are the protons of MQ[26]. In addition, it can be inferred by integrating the area calculation that the molar ratio of MQ and St in the polymer is about 1:10. According the ^{1}H NMR spectra of copolymer PNIPAM and block polymer PNIPAM-*b*-P(St-*co*-MQ), the average molecular weights of two polymers are calculated to be about 20.1 and 29 kDa, which is similar with the GPC results (see Table 1: $M_{n,GPC}$=21.0 kDa and 30.1 kDa). So the structure of two polymers synthesized by us can be denoted as $PNIPAM_{177}$ and $PNIPAM_{177}$-b-$P(St_{0.91}$-co-$MQ_{0.09})_{75}$.

FTIR can provide an additional evidence for the conjugation of PNIPAM and PNIPAM-*b*-P(St-*co*-MQ). As shown in Figure 3a, the characteristic peak at 1646 and 1538 cm^{-1} are ascribed to the existence of the stretching vibrations of C=O bands (amide I and II band) and the others (2864, 2922 and 2968 cm^{-1}) are related to the fundamental stretching vibration of -CH(CH_3)$_2$[28]. In the spectrum of block polymer PNIPAM-*b*-P(St-*co*-MQ) (see Figure 3b), some new bands appear at 1781, 2939, 2985, 3043 and 710cm^{-1}. Among them, the typical peak at 1781 cm^{-1} which is the characteristic peak of MQ units(C=O vibration)[26] and the bands appear at 3043, 2985, 2939 and 710 cm^{-1} correspond to the characteristic peaks of benzene in

Preprints (www.preprints.org) | NOT PEER-REVIEWED | Posted: 15 April 2022 doi:10.20944/preprints202204.0140.v1

polystyrene molecules[29]. In short, FTIR spectral analyses verify that the efficient polymerization of PNIPAM and PNIPAM-*b*-P(St-*co*-MQ).

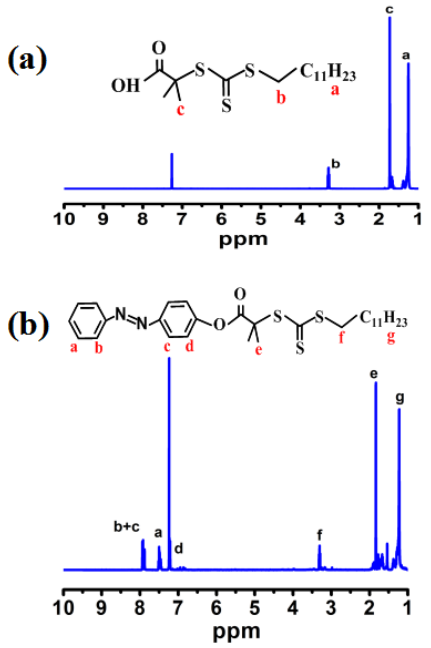

Figure.1 ^{1}H NMR spectra of RAFT (a) and azobenzene-RAFT (b).

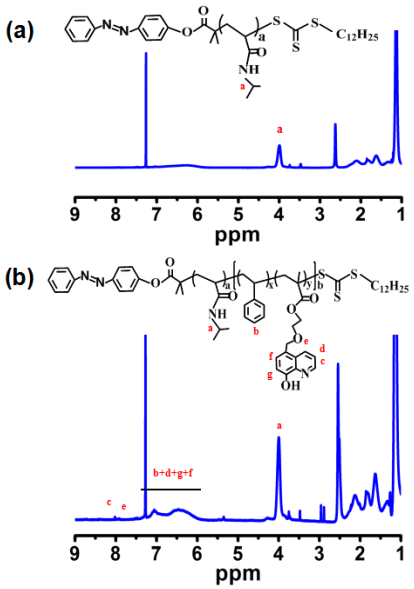

Figure.2 ^{1}H NMR spectra of PNIPAM (a) and PNIPAM-b-P(St-co-MQ) (b).

Table 1 Characterization data of polymer synthesized by RAFT polymerization.

Polymer	M_{NMR}※	M_n	M_w	PDI
$PNIPAM_{177}$	20.1	21.0	32.0	1.37
$PNIPAM_{177}$-b-$P(St_{0.91}$-co-$MQ_{0.09})_{75}$	29.0	30.1	45.5	1.37

※ M_{NMR} were calculated on the basis of ^{1}H NMR results.

Preprints (www.preprints.org) | NOT PEER-REVIEWED | Posted: 15 April 2022 doi:10.20944/preprints202204.0140.v1

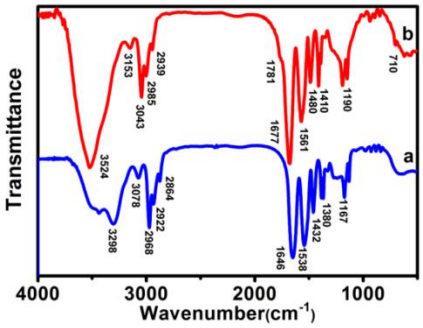

Figure 3 FTIR spectra of PNIPAM (a) and PNIPAM-b-P(St-co-MQ) (b).

Figure 4 is the Raman spectrum of GO and QDs/polymer/GO fluorescence nanohybrid. As shown in Figure 4, there are two obvious bands at 1337 and 1609 cm^{-1}. the band at 1337 cm^{-1} which be named as D band is link to the vibration of carbon atoms with dangling bonds in plane terminations of disordered graphite, confirming the formation of sp^3 carbon in GO. while the band at 1609 cm^{-1} which be named as G band and corresponding an E_{2g} mode of graphite was assigned to the number of sp^2 carbon atoms[28-30]. On the other hand, the intensity ratio of D and G bands (I_D/I_G) is the common data which used to characterize the defect density of graphene[30]. For our samples, the I_D/I_G ratios of the GO is about 1.13 while the QDs/polymer/GO fluorescence nanohybrid enhance to 1.16. This interesting phenomenon should be attributed to the gradual increase of sp^3 carbon structure after polymerization[28, 29]. Furthermore, we could calculate the size of sp^2 carbon clusters of GO and QDs/polymer/GO fluorescence nanohybrid by the Knights empirical formula[31]:

$$L_a=4.35/(I_D/I_G) \quad (1)$$

where L_a is stand for the size of sp^2 carbon clusters, and the intensity ratio between D and G band can be sighed as I_D/I_G . In this work, the sizes of sp^2 carbon clusters (L_a) of GO and the fluorescence nanohybrid are 3.85 and 3.75 nm respectively. It is confirmed that the block polymer and QDs modified on the surface of GO result a gradual reduction of graphitic structure which lead to an increase of I_D/I_G ratio and a decrease of the size of the graphitic domains[28-30].

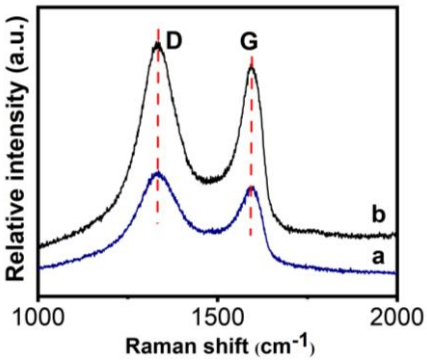

Figure 4 Raman spectra of GO (a) and QDs/polymer/GO fluorescence nanohybrid (b).

 doi:10.20944/preprints202204.0140.v1

The morphology of GO, CdSe/ZnS QDs, CD-GO and QDs/polymer/GO fluorescence nanohybrid were characterized by TEM. As depicted in Figure 5a, many of wrinkles and folding are displayed in the pristine GO, which seems as an exfoliated crumpled thin flake[28].The TEM images collected from the purchased CdSe/ZnS QDs is shown in Figure 5b. As seen from Figure 5b, the CdSe/ZnS QDs with a diameter of about 8-10 nm and its internal lattice fringes can be clearly observed, indicating that the quantum dot has a good lattice structure. After modified with β-cyclodextrinon though amidation(see Figure 5c), it is obviously that the monolayer GO sheet becomes thicker and the wrinkles and folding disappear, the appearance of dark areas indicate that β-cyclodextrinon has been modified on the surface of GO[26]. From the TEM images of QDs/polymer/GO fluorescence nanohybrid(see Figure 5d), we can clearly observe that the thin homogeneous polymer layer on the surface of GO with the dark area over the GO sheets. In addition, the CdSe/ZnS QDs are enwrapped by the polymer brushes with 8-hydroxyquinoline ligands on the side chains via the coordination interaction in the dried state for the sample preparation of TEM testing.The above TEM results imply that the block copolymer PNIPAM-b-P(St-co-MQ) has been anchored onto the surface of the GO by host-guest recognition and the 8-hydroxyquinoline ligands in the block copolymer has coordinated with CdSe/ZnS QDs successfully.

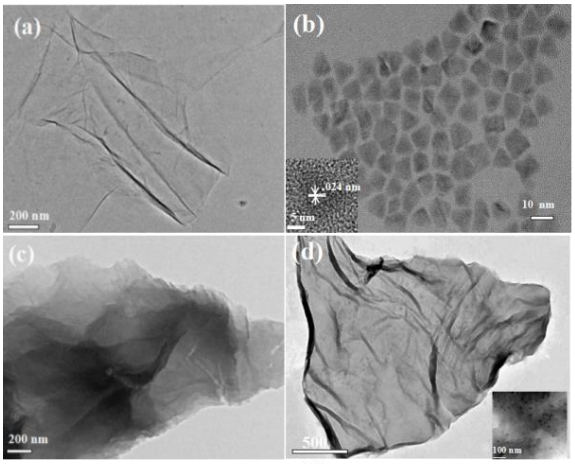

Figure 5 TEM images of GO (a), CdSe/ZnS QDs (b), GO-CD (c) and fluorescence nanohybrid (d).

TGA analysis was carried out to study the thermal stability of GO and QDs/polymer/GO nanohybrid. As presented in Figure 6a, the first small mass loss (15 wt %) of GO below 150 ºC is corresponding to the volatilization of physically absorbed water[32]. The GO was found to have approximately 50 wt% weight loss(except water) in the range of 200-600 ºC, which result from the thermal decomposition of liable oxygen-containing groups on its π-stacked structure[28-30]. From the TGA curves of QDs/polymer/GO nanohybrid(seen Figure 6b), the decomposed weight fraction of block copolymer brushes is about 85 wt% when the temperature was elevated from 200 ºC to 490 ºC. As shown in Figure 6c, the thermal stability of free block copolymer is higher than that of GO obviously, which illustrate that the thermal stability of GO can be enhanced with block copolymer.

Preprints (www.preprints.org) | NOT PEER-REVIEWED | Posted: 15 April 2022 doi:10.20944/preprints202204.0140.v1

Though the host-guest interaction to some extent and the TGA curve of QDs/polymer/GO nanohybrid proves this conclusion. On the other hand, the grafting density of PNIPAM-b-P(St-co-MQ) can be calculate from the formula according to TGA analysis as follow[33]:

$$\tilde{A}_{mg} = \frac{M_C W_F}{M_F W_C} \quad (2)$$

where M_C is the relative molar mass of carbon (M_C =12 g mol^{-1}), M_P is the average molecular weight (M_n) of modified polymer (come from GPC), W_C is the weight fractions of the block copolymer modified graphene backbone (not including grafted polymer) while W_p is the weight fractions of the grafted polymer. Therefore, based on the TGA curves of GO and QDs/polymer/GO nanohybrid as well as GPC measurement, the grafting density of PNIPAM-*b*-P(St-*co*-MQ) chains on GO sheets can be calculated to be 1.1 chains per 100 carbons in this work.

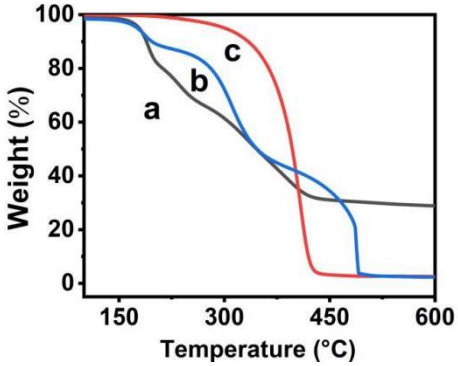

Figure 6 TGA curves of GO(a),fluorescence nanohybrid(b) and PNIPAM-b-P(St-co- MQ)

3.2 Optical properties of QDs/polymer/GO fluorescence nanohybrid

Figure 7 is the UV-vis absorption spectra of GO and QDs/polymer/GO fluorescence nanohybrid, The inset is the UV-vis absorption spectrum of CdSe/ZnS QDs. As shown in Figure 7a, GO has an absorption peak at 230 nm which is associated with the π-π* transition of aromatic C=C bond, and the absorption at 300 nm can be assigned to the n-π* transition of C=O bonds[34]. After functionalized with block copolymer PNIPAM-*b*-P(St-*co*-MQ) and CdSe/ZnS QDs(see Figure 7b), a new absorption peak can be observed at 249 nm which is caused by the the π-π* electron transition from quinoline ring[35], while another absorption can be seen at 352 nm which is resulted from the metal-quinolate transition in PNIPAM-*b*-P(St-*co*-MQ)[36]. Besides, in the spectra of QDs/polymer/GO fluorescence nanohybrid, the typical characteristics of CdSe/ZnS QDs at 620 nm can not be observed obviously, this phenomenon should be attributed to the characteristic absorption of the CdSe/ZnS QDs is too small as compared with the absorption from the QDs-quinolate transition.

 doi:10.20944/preprints202204.0140.v1

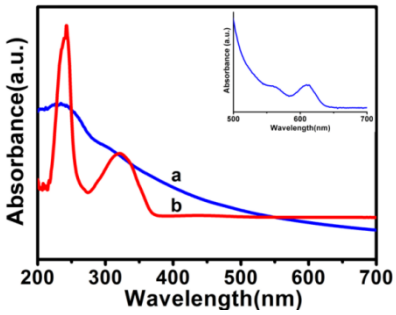

Figure 7 UV-vis absorption spectra of GO(a),QDs/polymer/GO(b)and CdSe/ZnS QDs(inset).

Figure 8 is the fluorescence spectrum of CdSe/ZnS QDs and QDs/polymer/GO fluorescence nanohybrid. As seen in Figure 8a, the CdSe/ZnS QDs have a distinct red-light emission at 620 nm as excited by 380 nm at room temperature. While the CdSe/ZnS QDs coordinated with 8-hydroxyquinoline units containing in the block copolymer on the surface of GO, there are two obvious emission centers, the emission at 620 nm orginates from the inherent luminescent emission of CdSe/ZnS QDs and annother strong green-light emission at 526 nm results from the surface-coordination emission between Zn^{2+} containing in the CdSe/ZnS QDs and 8-hydroxyquinoline containing in the block copolymer. As result, the QDs/polymer/GO fluorescence nanohybrid we prepared in this work shows two-channel fluorescence emission.

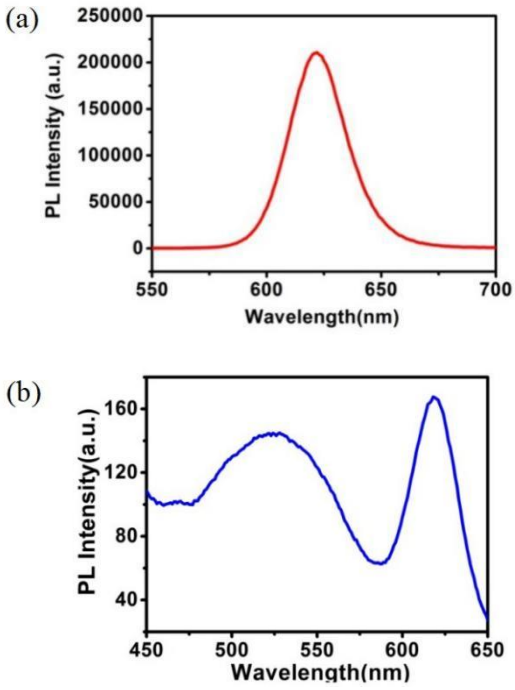

Figure 8 PL of CdSe/ZnS QDs (a) and QDs/polymer/GO fluorescence nanohybrid (b).

 doi:10.20944/preprints202204.0140.v1

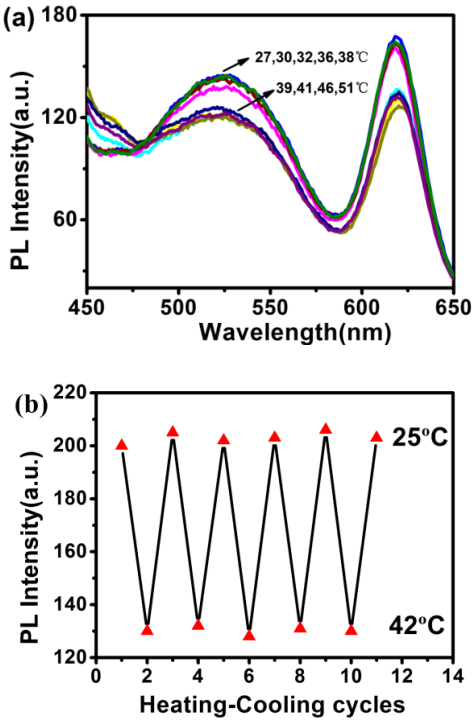

Figure 9 Evolution of fluorescence spectra as a function of temperature for QDs/polymer/GO fluorescence nanohybrid(a) and corresponding cycles of heating-cooling at above and below LCST of QDs/polymer/GO(b).

Owing to the incorporation of PNIPAM from the block polymer, the GO based fluorescence nanohybrid become readily dissolved in water under sonication. So the temperature-dependent fluorescence property of QDs/polymer/GO fluorescence nanohybrid was performed in water. Figure 9a depicts a nice change of fluorescence intensity with the temperature change and show a sharp increase at 38 °C. the fluorescence emission of QDs/polymer/GO fluorescence nanohybrid was quenched with the temperature increased from 39 °C to 51 °C. This interesting phenomenon should be put down to the different microenvironment caused by the conformation change of PNIPAM in the response to the different temperature[16,37,38]. Actually, when the temperature below 38 °C, the luminescence intensity increases evidently for the fluorescence nanohybrid, which should be ascribed to the PNIPAM chains became hydrophilic below its LCST and exhibited expanded chain conformation. under this circumstances, the distance between the QDs and GO surface increases, suppressing the fluorescence resonance energy transfer (FRET) between the donor and acceptor.While the temperature of the aqueous solution is above 38 °C, the distance between the QDs and GO surface decreases. The luminescence from the emission center, however, is not completely quenched in this aqueous solution, the reason is that the sufficient distance between GO and QDs which modified on the block polymer still provides by the globule state of PNIPAM chains. Furthermore, the reversibility of the thermo-response of QDs/polymer/GO fluorescence nanohybrid was also discussed. As shown in Figure 9 b, ten continuous cycles of the

 doi:10.20944/preprints202204.0140.v1

efficient on-off switching behaviour happen in the GO hybrid aqueous solution. Though cooling the sample solution, the quenched fluorescence could be recovered completely. When re-heated above LCST, the GO based fluorescence nanohybrid performs the similar PL quenching efficiency. The above study indicate that there is a strong interaction between the thermo-responsive block copolymer and GO sheets, which induced the high stability.

4. Conclusions

In conclusion, the Azo-terminated block polymer PNIPAM-b-P(St-co-MQ) has been functionalized on the surface of β-cyclodextrin modified GO via host-guest interaction successfully. What's more, the 8-hydroxyquinoline units containing in the block polymer could coordinate with CdSe/ZnS QDs to fabricate a QDs/polymer/GO fluorescence nanohybrid. The QDs/polymer/GO fluorescence nanohybrid had a robust temperature responsive property which result from the change in the PNIPAM conformation in the block copolymer on the surface of GO. Hence, considering the extensive potential applications of GO as a host material for a variety of copolymer and nanoparticles, the design developed here could be an effective strategy for producing carefully designed GO-polymer-active nanoparticles fluorescent hybrids for optical, electronic, catalysis, environment and new energy fields.

Author Contributions: Conceptualization, H.L.; methodology, J.L.; software, H.Y.; validation, X.W.,H.L. and J.L.; formal analysis, Y.S.and H.Y.; investigation,Y.S. and H.Y.; resources, H.L.; data curation,Y.S.and X.W.; writing-original draft preparation,Y.S. and H.Y.; writing-review and editing, H.L. and J.L.; visualization,Y.S.; supervision, J.L.; project administration, Y.S., H.Y. and X.W.; funding acquisition, Y.S., H.Y. and X.W. All authors have read and agreed to the published version of the manuscript.

Funding: This research was funded by the Inner Mongolia Natural Science Foundation of China, grant number 2018BS02005 and 2019BS02009; Research Project of Colleges and Universities in Inner Mongolia Autonomous Region, grant number NJZY20116 and NJZY21418; and Doctoral Scientific Research Foundation of Inner Mongolia Minzu University, grant number BS397 and BS425.

Institutional Review Board Statement: Not applicable.

Informed Consent Statement: Not applicable.

Data Availability Statement: The data presented in this study are available upon request from thecorresponding author.

Acknowledgments: We would like to appreciate the financial support of the Inner Mongolia Natural Science Foundation of China, Research Project of Colleges and Universities in Inner Mongolia Autonomous Region, Doctoral Scientific Research Foundation of Inner Mongolia Minzu University.

Conflicts of Interest: The authors declare no conflict of interest.

References

1. Jirí cková, A.; Jankovský, O.;Sofer, Z.; Sedmidubský, D. Synthesis and applications of graphene oxide. *Materials*. **2022**, 15, 920.
2. Novoselov, K. S.; Geim, A. K.; Morozov, S. V.; Jiang, D.; Katsnelson, M. I.; Grigorieva, I. V.; Dubonos, S. V. Two-dimensional gas of massless dirac fermions in graphene. *Nature*, **2005**, 438, 197-200.
3. Stankovich, S.; Dikin, D. A.; Dommett, G.; Kohlhaas K. M.; Zimney,E. J.; Stach, E. A.; Piner, R. D.; Nguyen S. B.; Ruoff,R. S. Graphene-based composite material. *Nature.* **2006**, 20, 282-286.
4. Guo,S.; Garaj, S.; Bianco,A; Moyon, C. M. Controlling covalent chemistry on graphene oxide. *Nature Reviews Physics*. **2022**,4,247-262.
5. Marsden, A. J.; Skilbeck, M.; Healey, M.; Thomas, H. R.; Walker, M.; Edwards, R.S.; Garcia, N.A.; Vukovic, F.; Jabraoui, H.; Walsh, T. R.; Rourke, J. P.; Wilson, N. R. *Phys. Chem. Chem. Phys*. **2022**, 24, 2318-2331.
6. Costa, M. C. F.; Marangoni, V. S.; Ng, P. R.; Nguyen, H.T. L.; Carvalho, A.; Castro Neto, A. H. Accelerated synthesis of graphene oxide from graphene. **2021**, 11, 551-559.
7. Sinha, A.; Ranjan, P.; Thakur, A. D. Effect of characterization probes on the properties of graphene oxide and reduced graphene oxide. *Applied Physics A*. **2021**, 127, 585-598.
8. Singh,R.; Ullah, S.; Rao, N.; Singh, M.; Patra, I.; Darko, D.A.; C. Issac, P. J.; Salestani, K. E.; Kanaoujiya, R.; Vijayan, V. Synthesis of three-dimensional reduced-graphene oxide from graphene oxide. *Journal of Nanomaterials*. **2022**, 8731429.
9. Kumar, N.; Setshedi, K.; Masukume1, M.; Sinha Ray, S. S. Facile scalable synthesis of graphene oxide and reduced graphene oxide: comparative investigation of diferent reduction methods. *Carbon Letters*. **2022**, 28.
10. Zhang,L.; Xia, J. G.; Zhao, Q. H.; Liu, L. W.; Zhang, Z. J. Functional graphene oxide as a nanocarrier for controlled loading and targeted delivery of mixed anticancer drugs. *Small*, **2010**, 6, 537-544.
11. Layek,R. K.; Nandi, A. K. A review on synthesis and properties of polymer functionalized Graphene. *Polymer*, **2013**, 54, 5087-5103.
12. Zhang, B.; Chen, Y.; Xu, L. Q.; Zeng, L. G.; He, Y.; Kang, E. Y.; Zhang, J. J. Growing poly(N-vinylcarbazole) from the surface of graphene oxide via RAFT polymerization. *J. Polym. Sci., Part A: Polym. Chem.*, **2011**, 49, 2043-2050.
13. Liu,J. Q.; Yang, W. R.; Tao, L.; Li, D.; Boyer, C.; Davis, T. P. Thermosensitive graphene nanocomposites formed using pyreneterminal polymers made by RAFT polymerization. *J. Polym. Sci., Part A: Polym. Chem.*, **2010**, 48, 425-433.
14. Salavagione, H. J.; Gómez, M. A.; Martínez, G. Polymeric modification of graphene through esterification of graphite oxide and poly(vinylahcohol). *Macromolecules*, **2009**, 42, 6331-6338.

15. Liu, Z. Robinson, J. T.; Sun, S. M.; Dai, H. G. PEGylated nanographene oxide for delivery of water-insoluble cancer drugs. *J. Am. Chem. Soc*. **2008**, 130, 10876-10877.
16. Pan, Y. Z.; Bao, H. Q.; Sahoo, N. J.; Wu, T. F.; Li, L. Water-soluble poly(N-isopropylacry lamide)-graphene sheets synthesized via click chemistry for drug delivery. *Adv. Funct. Mater*., **2011**, 21, 2754-2763.
17. Yang, H.; Paek, K.; Kim, B. J. Efficient temperature sensing platform based on fluorescent block copolymer-functionalized graphene oxide. *Nanoscale*, **2013**, 5, 5720-5724.
18. Li, W.F.; Liang, J. Y.; Yang, W. T.; Deng J. P. Chiral Functionalization of Graphene Oxide by Optically Active Helical-Substituted Polyacetylene Chains and Its Application in Enantioselective Crystallization. *ACS Appl. Mater. Interfaces*. **2014**, 6, 9790−9798.
19. Vuluga, D.; Thomassin, J. M.; Molenberg, I.; Huynen, I.; Gilbert, B.; Detrembleur, C. Straightforward synthesis of conductive graphene/polymer nanocomposites from graphite oxide. *Chem. Commun*. **2011**, 47, 2544-2546.
20. Huang, H. D.; Liu, C. Y.; Li, D.; Chen, Y. H.; Zhong, J. G.; Li, Z. M. High performance of electrochemical lithium storage batteries: ZnO-based nanomaterials for lithium-ion and lithium-sulfur batteries. *J. Mater. Chem. A*. **2014**, 2, 15853-15859.
21. Paek, K.; Yang, H.; Lee, J.; Park J.; Kim, B. J. Efficient colorimetric pH sensor based on responsive polymer quantum dot integrated graphene oxide. *ACS Nano*, **2014**, 8, 2848-2856.
22. Jiang, K.; Ye, C.; Zhang, P. P.; Wang, X. S.; Zhao, Y. L. One-pot controlled synthesis of homopolymers and diblock copolymers grafted graphene oxide using couplable RAFT agents. *Macromolecules*. **2012**, 45, 1346−1355.
23. Shi, Y. G.; Liu, M. Y.; Wang, K.; Deng, F. J.; Wan, Q.; Huang, Q.; Fu, L. H.; Zhang, Y. X.; Wei, X. Bioinspired preparation of thermo-responsive graphene oxide nanocomposites in an aqueous solution. *Polym. Chem*. **2015**, 6, 5876-5883.
24. Hummers,W. S.; Offeman, R. E. Preparation of graphitic oxide. *J. Am. Chem. Soc*., **1958**, 80, 1339.
25. Ferguson,C. J.; Hughes, R. J.; Nguyen, D.; Pham, B. T.; Gilbert, R. G.; Serelis, A. K.; Such C. H.; Hawkett, B. S. Ab initio emulsion polymerization by RAFT-controlled self-assembly. *Macromolecules*, **2005**, 38, 2191-2204.
26. Du, N. Y.; Tian, R. Y.; Peng, J. B.; Lu, M. Synthesis and photophysical characterization of the free-radical copolymerization of metaloquinolate-pendant monomers with methyl methacrylate. *J. Polym. Sci. Pol. Chem*., **2005**, 43, 397-406.
27. Li, Y.; Gao, Y.; Li Y.N.; Liu S. Y.; Zhang, H, Su, X. G. A novel fluorescence probing strategy based on mono-[6-(2-aminoethylamino)-6-deoxy]-cyclodextin functionalized graphene oxide for the detection of amantadine. *Sensors and Actuators B*. **2014**, 202, 323-329.
28. Liu, J. H.;Chen, G. S.; Guo, M. Y.; Jiang M. Dual stimuli-responsive supramolecular hydrogel based on hybrid inclusion complex (HIC). *Macromolecules*. **2010**, 43, 8086-8093.
29. Kundu, A.; Nandi, S.; Das, P.; Nandi, A. K. Fluorescent graphene oxide via polymer grafting: an efficient nanocarrier for both hydrophilic and hydrophobic drugs. *ACS Appl. Mater. Interfaces*. **2015**, 7, 3512−3523
30. Ding, P.; Zhang, J.; Song, N.; Tang, S. F.; Liu, Y. M.; Shi, L. Y. Growing polystyrene chains from the surface of graphene layers via RAFT polymerization and the influence on their thermal properties. *Composites: Part A*. **2015**, 69, 186-194.

31. Zhang, Q.; Li, Q. L.; Xiang, S.; Wang, Y.; Wang, C.; Jiang, W.; Zhou, H.; Yang, Y. W.; Tang, J. Covalent modification of graphene oxide with polynorbornene by surface-initiated ring-opening metathesis polymerization. *Polymer*, **2014**, 55, 6044-6050.
32. Diane S.; Knight; William B.;White. Characterization of diamond films by Raman spectroscopy. *J. Mater. Res.***1989**, 4,385-393.
33. Ye, Y. S.; Chen, Y. N.; Wang, J. S.; Rick, J.; Huang, Y. J.; Chang F. C.; Hwang, B. J. Versatile grafting approaches to functionalizing individually dispersed graphene nanosheets using RAFT polymerization and click chemistry. *Chem. Mater*. **2012**, 24, 2987-2997.
34. Wallace, G.G.; Kaner, R. B.; Muller, M.; Gilje, S.; Li, D. Processable aqueous dispersions of graphene nanosheets, Nat Nanotechnol., **2008**, 3, 101-105.
35. Liu, B. X.; Tong, C. Y.; Feng, L. J.; Wang, C. Y.; He, Y.; Lü, C. L. Water-Soluble Polymer Functionalized CdTe/ZnS Quantum Dots:A Facile Ratiometric Fluorescent Probe for Sensitive and Selective Detection of Nitroaromatic Explosives. *Chem. Eur. J*., **2014**, 20, 2132-2137.
36. Bolívar, C. P.; Takizawa, S. Y.; Nishimura, G.; Montes, V. A.;Jr, P. A. High-Efficiency tris (8-hydroxyquinoline)aluminum (Alq_3) complexes for organic white-light-emitting diodes and solid-state lighting. *Chem. Eur. J*. **2011**, 17, 9076-9082.
37. Liu, C. H.; Wang, Z.; Jia, H. X.; Li, Z. P. Efficient fluorescence resonance energy transfer between upconversion nanophosphors and graphene oxide: a highly sensitive biosensing platform. *Chem. Commun*. **2011**, 47, 4661-4663.
38. Xie, L. M.; Ling, X.; Fang, Y.; Zhang, J.; Liu, Z. F. Graphene as a substrate to suppress fluorescence in resonance raman spectroscopy. *J. Am. Chem. Soc*. **2009**, 131, 9890-9891.